[Epigenetics 1:4, 155-162, October/November/December 2006]; ©2006 Landes Bioscience

Research Paper

# In Vivo Methylation Patterns of the Leptin Promoter in Human and Mouse

**Reinhard Stöger**

Correspondence to: Reinhard Stöger; Department of Biology; University of Washington; Box 351800; Seattle, Washington 98195-1800 USA; Tel.: 206.616.9385; Fax: 206.543.3041; Email: stoeger@u.washington.edu

Original manuscript submitted: 07/19/06
Manuscript accepted: 09/13/06

Previously published online as an *Epigenetics* E-publication:
http://www.landesbioscience.com/journals/epigenetics/abstract.php?id=3400

**KEY WORDS**

methylation density, promoter methylation, metabolic gene, leptin, T-DMR

**ABBREVIATIONS**

| | |
|---|---|
| PBLs | peripheral blood leukocytes |
| T-DMR | tissue-specific differentially methylated region |

**ACKNOWLEDGEMENTS**

I thank Charles Laird for continuous support and suggestions of data analysis, Diane Genereux for doing the two-sample Kolmogorov-Smirnov test, Lisa Chakrabarti, Diane Genereux and Alice Burden for helpful comments on the manuscript. Mouse epididymis cells were a gift from Sandy Baccam. Funds of NIH Grants GM53805 and HD02247 supported this work.

## ABSTRACT

Leptin is a fat hormone regulating energy homeostasis. Here, it is reported that the promoter and CpG island of the autosomal gene *Leptin* (*LEP*) is a tissue-specific differentially methylated region (T-DMR) and subject to dynamic methylation in human and mouse in vivo. Highly variable densities of cytosine methylation were detected by hairpin-bisulfite PCR among cells in human adipose tissue and peripheral blood leukocytes. Intermediate and low levels of methylation characterize the majority of human *LEP* epialleles. Low-density epialleles are often methylated at a specific CG site within the binding element of the C/EBP-α transcription factor. In the human *LEP* promoter, the methylation frequency at that site is 1.8-fold as great as the average frequency for all other CG sites analyzed. The *Lep* promoter has a significantly higher methylation density in mouse somatic tissues than in the human *LEP* promoter. Though the *LEP* CpG island is generally unmethylated in both human and mouse sperm, depletion of CG sites within the mouse promoter indicates occasional presence of methylated *Lep* epialleles in the germline. These findings suggest that *LEP* promoter methylation is normally imposed during postzygotic development, and that this epigenetic mark may play a role in modulating expression of an important metabolic gene.

瘦素是一种调节能量稳态的脂肪激素. 在这里, 我们报道了染色体基因瘦素(LEP)的启动子和 CpG 岛是组织特异性甲基区, 它们在人和小鼠体内可发生动态甲基化. 我们通过亚硫酸盐修饰双链 PCR 扩增的方法探测到人类脂肪组织和外周血白细胞中不同密度的胞嘧啶甲基化. 中度和低度甲基化是大部分主要人类 LEP 表观等位基因的特性. 低密度的表观等位基因甲基化经常发生在 C/EBP-alpha 转录子的结合区. 在人类 LEP 启动子, C/EBP-alpha 转录子的结合区甲基化的频率是其它被分析的 CG 位点的平均频率的 1.8 倍. LEP 启动子在小鼠体组织中甲基化的密度要显著高于在人类 LEP 启动子中的密度. 尽管在人和小鼠精子里的 CpG 岛一般都是未甲基化的, 但在小鼠启动子内 CG 位点的耗尽显明了在生殖系中有甲基化的 LEP 表观等位基因的偶尔存在. 这些发现表明 LEP 启动子的甲基化通常被强加在合子后发育中, 这种表现基因型标记可能在调节一种重要的代谢基因的表达上有作用.

## INTRODUCTION

Methylation is a nucleotide modification which, in mammalian DNA, is primarily confined to cytosines of 5'-CG-3' dinucleotides. These potential sites of cytosine methylation are not uniformly distributed within the genome. Domains with a high density of 5'-CG-3' dinucleotides, also termed CpG islands, punctuate the mammalian genome that is otherwise characterized by a relative depletion of CGs based on the GC content.[1-4] CpG islands frequently harbor promoters and first exons of genes.[3] Genome analysis suggests that transcription of about 75% of genes is controlled and initiated within CG-rich regions.[4-6] It is generally assumed that most CpG islands associated with gene promoters remain completely unmethylated throughout development, and in all tissues of an animal. However, based on data form recent genomic studies on mouse tissues, it has been estimated that as many as 5%-34% of CpG islands constitute tissue-specific differentially methylated regions (T-DMRs).[7-9] Although the genetic information of T-DMRs is identical between tissues and cells of an individual, differences in cytosine methylation patterns generate epigenetic variants, which I refer to as "epialleles".

Dense promoter methylation is highly correlated with heritable gene-silencing,[10-12] (reviewed in ref. 13). The best-documented examples are methylated CpG islands on the inactive X-chromosome in females, and genomic regions that carry a parental-specific imprint. In both cases, CpG island-methylation has evolved as a developmentally regulated mechanism participating in the process of reducing the dosage of a gene product by allelic silencing (reviewed in refs. 13–15).

Leptin, the product of the *obese* gene *Leptin (LEP)* is a key hormone regulating energy intake and expenditure,[16] (reviewed in ref. 17). The *LEP* promoter is embedded within a CpG island (Fig. 1A). 217 base pairs containing a TATA-box element and a functional

C/EBP-α binding site are sufficient for tissue-specific gene expression.[18,19] The core of the binding sequence for transcription factor C/EBP-α in the *LEP* promoter contains a CG dinucleotide, a possible site for cytosine methylation (see Fig. 1B).

Methylation of the *LEP* promoter has been observed in a mouse and a human cell line, both of which can be induced to differentiate into adipocytes.[20,21] Methylation data obtained from cell lines may not always reflect the in vivo methylation status of a particular locus, since CpG islands of nonessential genes frequently become methylated under tissue culture conditions.[22]

The aim of this study was to investigate whether the regulatory region of *LEP*, an autosomal gene not known to carry a parental-specific imprint, is methylated in human and mouse tissues. Here, I establish that the *LEP* promoter is indeed methylated in both species. The properties of these methylation patterns are described.

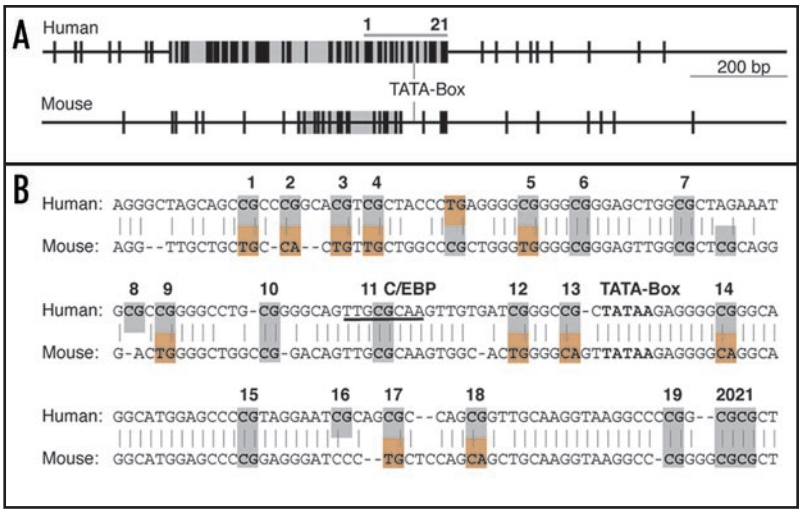


Figure 1. The human and mouse *Leptin* promoters. (A) Plots show the distribution of CG dinucleotides - potential sites of cytosine methylation - within a 1.5 kb genomic region centered around the TATA-box promoter element. DNA segments meeting criteria of CpG islands are depicted in gray; defining criteria are described in the Methods section. (B) Alignment of the core *Leptin* promoter sequence from human and mouse. CG dinucleotides are highlighted in gray, while TG or CA nucleotide substitutions are highlighted in bown. The methylation status of 21 CG sites was analyzed on the human promoter.

## MATERIALS AND METHODS

**Criteria used to define the LEP/Lep CpG islands.** percentage of Cs and Gs >60%; ratio of observed to expected CG dinucleotides >0.7; size of CpG island sequence >200 nucleotides. DNA sequence information of the mouse and human CpG islands, including flanking sequences was obtained via the UCSC Genome Browser created by the Genome Bioinformatics Group of UC Santa Cruz: (http://genome.ucsc.edu/cgi-bin/hgGateway). The position of the human *Leptin* CpG island is: Chromosome 7: 127474702-127475326; The position of the mouse *leptin* CpG island is: Chromosome 6: 28992101-28992316.

**CpG island plots/CG distribution.** plots generated by the online "MethPrimer" program (www.urogene.org/methprimer/index1.html) were used as templates to draw the CG distribution with "Adobe Illustrator" software.

**Sequence alignment.** Figure 1B shows the result of two sequence alignments: Alignment of mouse and human *Leptin* promoter sequences covering human CG sites 1 to 4 was obtained from the comparative genome feature of the UCSC Genome Browser http://genome.ucsc.edu/cgi-bin/hgGateway (Alignment block 4 of 14 in window, 127668353-127668950, 598 bps at the *Leptin* locus). This alignment was merged with the results of a "2 sequence" BLAST (see following description). The sequences covering human CG sites 5 to 21 were aligned with the "BLAST 2 sequences" program (www.ncbi.nlm.nih.gov/blast/bl2seq/wblast2.cgi) using standard parameters (Open gap 5, and extension gap 2, penalties; gap x_dropoff 50; expect 10.0; word size 11 (www.ncbi.nlm.nih.gov/blast/newoptions.html - filter). The aligned sequences were edited using "Adobe Illustrator" software. Some gaps created by the two alignment programs were shifted between 1-2 nucleotide positions in order to get exact alignment between the human and mouse CG orthologues or their putative deamination products, respectively; this was done for sites 2, 10, 12, 13, 17 and 19.

**Tissues, cells and DNA.** Benign adipose tissues were provided by the Cooperative Human Tissue Network (CHTC), which is funded by the National Cancer Institute. Other investigators may have received specimens from the same subjects. Abdominal adipose tissues were obtained from individuals undergoing abdominoplasty. Female *F1*, 61 years of age, abdominoplasty; female *F3*, 42 years of age, abdominoplasty. Breast adipose tissues were obtained from individuals undergoing reduction mammoplasty. Female *F2*, 28 years of age, reduction mammoplasty; female *F5*, 18 years of age, reduction mammoplasty. For each individual sample approximately 5 x 5 mm of tissue with homogenous white adipose appearance was taken for DNA isolation using the standard QIAamp DNA Mini Kit protocol. DNA from PBLs (female *F10* and male *M3*) came from a collection of anonymous samples collected at the Seattle Children's Hospital; only the sex of the sample donors is known. The human sperm DNA sample came from a DNA collection of the Laird laboratory and had been isolated following a proteinase K, phenol/chloroform based protocol. The QIAamp DNA Mini Kit protocol was used to isolate DNA from white abdominal adipose tissue, spleen, liver and brain of adult (~12–18 months of age) mice. Mouse sperm cells were squeezed from the epididymis into a dish containing PBS buffer. Presence of adequate numbers of sperm cells was confirmed by use of the "Christmas Tree stain" which stains the sperm head red and the tails green. The protocol of the "Differex™ System" (Promega) was followed to enrich for mouse spermatozoa; it uses a combination of phase separation and differential centrifugation for the separation of sperm and "epithelial" (describing all cells that are not mature spermatozoa) cells. DNA was isolated and analyzed from both fractions (Fig. 6).

**Hairpin bisulfite PCR.** The hairpin bisulfite PCR method and protocol is described in detail.[23] In brief, ~5 μg of genomic DNA were cleaved with restriction enzymes close to the genomic region of interest: *NheI* for the human *Leptin* promoter; *StyI* (CG sites A–N), or *FokI* (CG sites M–U) for the mouse *leptin* promoter. After heat inactivation of restriction enzymes and buffer exchange, synthesized hairpin linkers were ligated onto the sticky ends of the cleaved genomic DNA. For each human DNA sample a hairpin linker with a different "batch-stamp" and "barcode" was used, thereby allowing the accruement of unambiguous sequence and methylation data and exclusion of redundant or contaminant sequences; the concept and use of encoded hairpin oligonucleotides has been described.[24] For

the spleen and brain DNA samples from mouse, the same hairpin linker was used (Fig. 5). Cytosine deamination by sodium bisulfite was performed as described.[23] Ten heat-denaturing steps were included during the sodium bisulfite incubation step to repeatedly denature the DNA and thereby achieve a very high degree (>99%) of C → U conversion of non-CG cytosines. Sequences with more than one unconverted non-CG cytosine were excluded from the data sets. Sequences of the human *Leptin* hairpin linkers are as follows: 5'-CTAGAGCGATGCDDDDDDDDGCATCGCT-3' for individual M1; 5'-CTAGAGCGTAGCDDDDDDDDGCTACG CT-3' for individual F10; 5'-CTAGACAGTGCADDDDDDDD TGCACTGT-3' for individual F1; 5'-CTAGGACGATGCDDDD DDDDGCATCGTC-3' for individual F2; 5'-CTAGACATGGCA DDDDDDDDTGCCATGT-3' for individual F3; 5'-CTAGATC GTGCADDDDDDDDTGCACGAT-3' for individual F4; 5'-CTA GAAGGTGCADDDDDDDDTGCACCTT-3' for individual F5; 5'-CTAGAGCGTAGCDDDDDDDDGCTACGCT-3' for individual F10; 5'-CTAGAGCGATCGDDDDDDCGATCGCT-3' for individual M1; 5'-CTAGAGGCATGCDDDDDDDDGCATGCC T-3' for individual M3. Sequences of the mouse *leptin* hairpin linkers are as follows: 5'-CTTGAGCGATGCDDDDDDGCATCGCT-3' for spleen and brain DNA samples; 5'-CTTGAGCGAAGGDDDD DDCCTTCGCT-3' for the liver DNA; 5'-TCTAAGCGATGCDD DDDDDDGCATCGCT-3' for mouse adipose DNA; 5'-TCTAAG CGTAGCDDDDDDDDGCTACGCT-3' for mouse brain DNA.

Primers to amplify the 464 nt human *Leptin* hairpin fragment from bisulfite converted genomic DNA: hlept-F: 5'-TGTTAAGA AAGATTAGTAGAGAAGGAGGA-3', hlept-R: 5'-AACCCTATAA CCTACCAAAAAAAAC-3'; annealing temperature: 53°C. Primers to amplify a 265 nt mouse *leptin* hairpin PCR fragment from bisulfite converted DNA to analyze CG sites A to D: hp-ob3F: 5'-TGGGGGYGTTTGGTATGAGTYG-3', hp-ob3R: 5'-ACAATA ACAACAACAACCTAATACTCC-3'; annealing temperature: 59°C. Primers to amplify a 435 nt mouse *leptin* hairpin PCR fragment from bisulfite converted DNA to analyze CG sites A to N: hp-ob2F: 5'-TTGTTYGGTTAGTTTTAGTTTTTGYGA-3', hp-ob2R: 5'-CRACCAACCCCAATCCCTAC-3'; annealing temperature: 53°C. Primers to amplify a 427 nt mouse *leptin* hairpin PCR fragment from bisulfite converted DNA to analyze CG sites M to U: obFokB-1F: 5'-GTTGTTATTGTTGTTGGTTYGTTG G-3', obFokB-ini: 5'-ATTACTACTACCACTATTACTAACC-3'; annealing temperature: 50°C. Typically, hairpin-PCRs were carried out in a reaction volume of 50 μl containing 25 μl HotStarTaq Master Mix (Qiagen), 1 μl each of forward and reverse primers (50 μM stock), 1–3 μl DMSO, 10–20 μl of bisulfite converted DNA and $H_20$ to adjust the reaction volume to 50 μl; 41 thermal cycles. PCR products were run on agarose gels, fragments isolated (QIAquick) and subsequently cloned (TOPO-TA cloning/Invitrogen). Sequencing of individual, cloned PCR products was carried out using the BIGDYE Terminator 3.0 sequencing kit (ABI) and run on ABI 3100 instrument.

**Conventional sodium bisulfite PCR.** was used to assess the methylation status of the mouse *leptin* promoter in sperm and epidermal DNA because only limited quantities of DNA were isolated. Thus, methylation information could only be obtained from the sense-strand (top-strand) of the promoter (Figs. 5 and 6). Less stringent conditions can be used to achieve C to U conversion and, therefore, less DNA is destroyed during the sodium bisulfite procedure. This in turn increases the chance of successful PCR amplification, as more un-nicked template DNA is present in the reaction. Only two denaturing cycles at 99°C were included during the bisulfite incubation step, which generated a conversion efficiency of 96–99%. Frequently one out of 27 non-CG cytosines failed to be converted in the recovered sequences from both the sperm and epidermal DNA samples. This enabled the identification and exclusion of redundant sequences. Sequences were deemed redundant if they had identical methylation patterns, but would also show failure of conversion at the same non-CG cytosine. Primers to amplify the 278 nt mouse *leptin* PCR fragment from bisulfite converted DNA to analyze CG sites L to U: bs-ob2F: 5'-TAGGTTGTTGTTGTTATT GTTGTTG-3', bs-ob-3R 5'-AACTATCCACATAACCTCCTTCT TAC-3'; annealing temperature: 58°C.

Stringent conditions were used to convert mouse adipose and liver DNA samples, resulting in >99% conversion of non-CG cytosines. Primers to amplify the 429 nt mouse *leptin* PCR fragment from bisulfite converted DNA to analyze CG sites A to U:

BS-OB1F: 5'-TTTTGGTTTATTGGTTTTTTTGTTT-3', BS-OB2R: 5'-CTATTAAAAAAACTAATAAAAAAAAAAATAAC-3': annealing temperature: 55°C.

Typically, PCRs were carried out in a reaction volume of 50 μl containing 25 μl HotStarTaq Master Mix (Qiagen), 1 μl each of forward and reverse primers (50 μM stock), 1–3 μl DMSO, 10–20 μl of bisulfite converted DNA and $H_20$ to adjust the reaction volume to 50 μl; 41 thermal cycles. Some of the PCR primers were designed using the online MethPrimer program (www.urogene.org/methprimer/index1.html).

**Chi-square test.** The Chi-square test was used to assess whether significant differences exist in *Leptin* promoter methylation densities between human and mouse. For this analysis data from epialleles that had 0, or 1 CG site methylated were excluded. The "0" class of epialleles was excluded because only methylated epialleles were examined; the "1" class of epialleles was excluded because a single methylation event lies within the range of "background noise" created by the occasional failure to convert an unmethylated cytosine during the sodium-bisulfite procedure. The remaining methylation data were pooled, independent of origin of tissue. For the human data pool a total of 4074 CG sites were sampled; 1246 methylation events were observed. For the mouse data pool a total of 1009 CG sites were sampled; 782 methylation events were observed.

## RESULTS AND DISCUSSION

The autosomal *LEP* gene is primarily expressed in differentiated adipocytes of white-fat tissue.[16] Therefore, in vivo methylation patterns of the human *LEP* CpG island were examined in benign abdominal and mammary fat tissue of females using hairpin bisulfite PCR. With this method, the methylation status can be determined on both strands of individual DNA molecules for all cytosines, including complementary, palindromic $^{5'\text{-CG-}3'}/_{3'\text{-GC-}5'}$ sites.[23] Each of the sampled genomic epialleles was tagged with a molecular batchstamp and barcode prior to the bisulfite sequencing procedure. This tagging ensures a high level of confidence in PCR-derived sequence data, since PCR contaminations and redundant epialleles can be identified and removed from the data set.[24] As expected, some epialleles are entirely unmethylated and likely derived from differentiated adipocytes expressing *LEP* (Fig. 2). However, most epialleles are methylated and show surprisingly large variation in methylation densities. The spectrum of methylation densities ranges from 2% (1/42) methylated CG dinucleotides, to 76% (32/42) (Fig. 2).

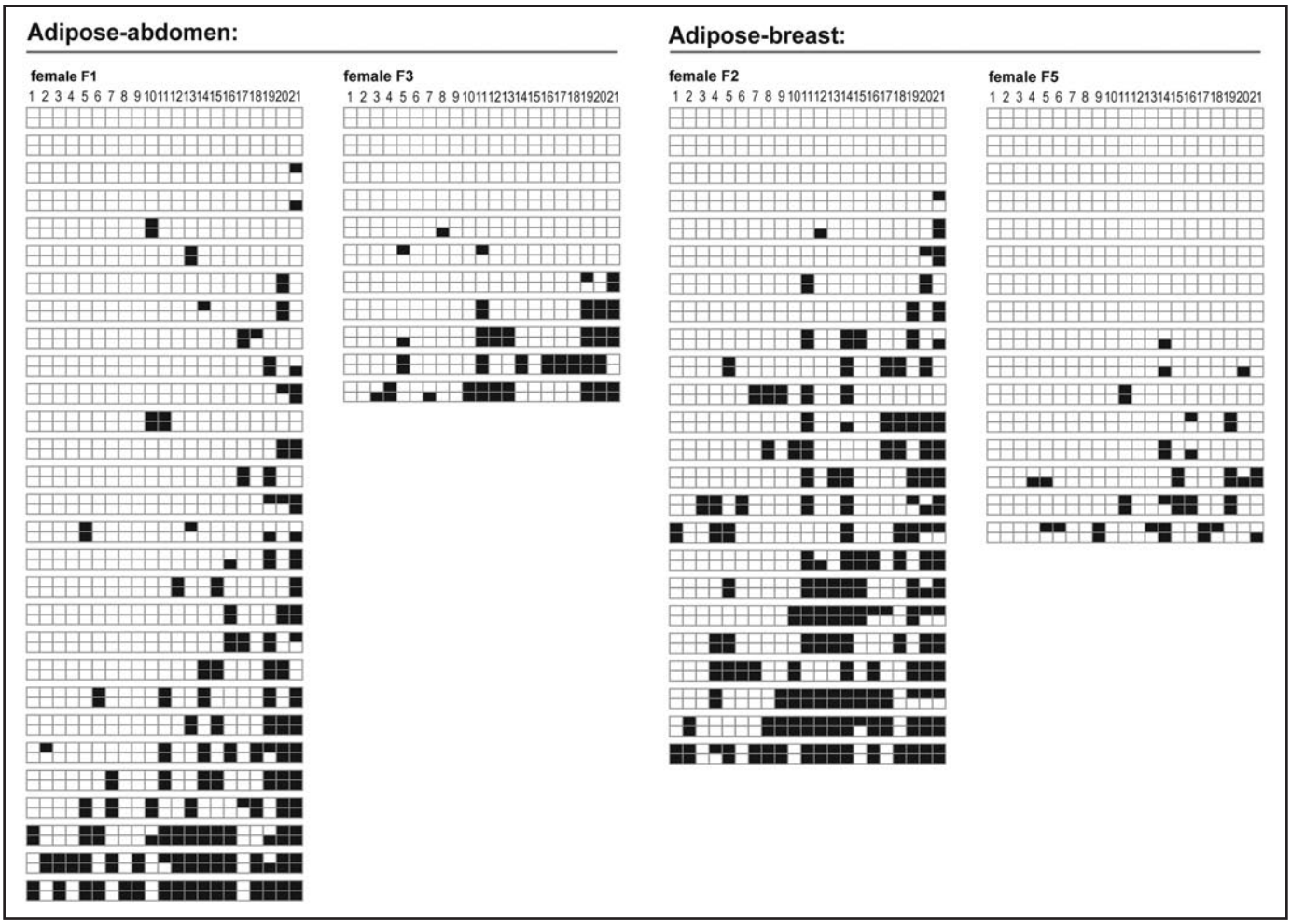


Figure 2. In vivo methylation patterns of the *LEP* promoter in human fat tissues. 21 complementary CG dinucleotides were analyzed by hairpin-bisulfite PCR on both strands of individual DNA molecules. The two rows of boxes within each rectangle represent CG sites on either the top or the bottom strand of an individual, double-stranded DNA molecule. Unmethylated CGs are shown in white; methylated CGs are shown in black. The sequences obtained from each tissue are sorted by methylation density. Numbers correspond with the 21 CGs of the human sequence depicted in Figure 1B.

The wide range of methylation densities at the human *LEP* promoter is unusual and differs from the bimodal methylation densities observed on genes carrying parental imprints, and from genes on the inactive X chromosome. Epialleles of both imprinted genes and inactive X genes have CpG islands that are either unmethylated and transcriptionally competent, or they are densely methylated and silenced[23,25,26] (see also Fig. 4). This type of methylation-bimodality is not unlike a control switch with two settings: "on" or "off". Once established, these epigenetic settings are stably maintained and inherited through many mitotic cell divisions. In contrast, low-density methylation, where only a subset of CG sites within a given locus is modified, appears to be inherently unstable.[27] Lorincz and colleagues, for example, used proviral reporter constructs in murine erythroleukemia cells and showed that reporter sequences with low-density methylation stochastically gave rise to bimodal populations composed of some unmethylated epialleles, and some densely methylated epialleles.[27] Consequently, it will be important to establish the origin and fate of moderately and sparsely methylated *LEP* epialleles. They may be derived from cells that stably maintain these low-density methylation levels, or, alternatively, from preadipocytes undergoing differentiation into mature adipocytes. In the latter case, these epialleles may be intermediates sampled during an epigenetic transition leading to a completely unmethylated *LEP* promoter. In vitro differentiation of preadipocytes to adipocytes indeed correlates with reduction of methylation at the promoter, and induction of *LEP* expression.[20,21] The question arises whether reduction of methylation density at the *LEP* promoter is a developmentally regulated process that occurs in vivo during adipocyte maturation. Methylation density is overall lower in epialleles recovered from fat tissue when compared with epialleles derived from peripheral blood leukocytes (see Figs. 2 and 3; and text below), supporting the hypothesis that *LEP* promoter demethylation may occur in adipose tissue. Various somatic cell types, including adipose tissue, will need to be sampled from one and the same individual in order to assess in greater detail the occurrence of tissue-specific demethylation.

To investigate the methylation status in different types of human somatic cells the same *LEP* promoter region was analyzed in peripheral blood leukocytes (PBLs). Pronounced diversity in methylation densities was observed, ranging from epialleles with 7% (3/42) CG methylation, to epialleles with 88% (37/42) methylated CG dinucleotides (Fig. 3). Only a single unmethylated epiallele was recovered from PBL DNA; intermediate levels of methylation characterize the majority of *LEP* epialleles (Fig. 4).

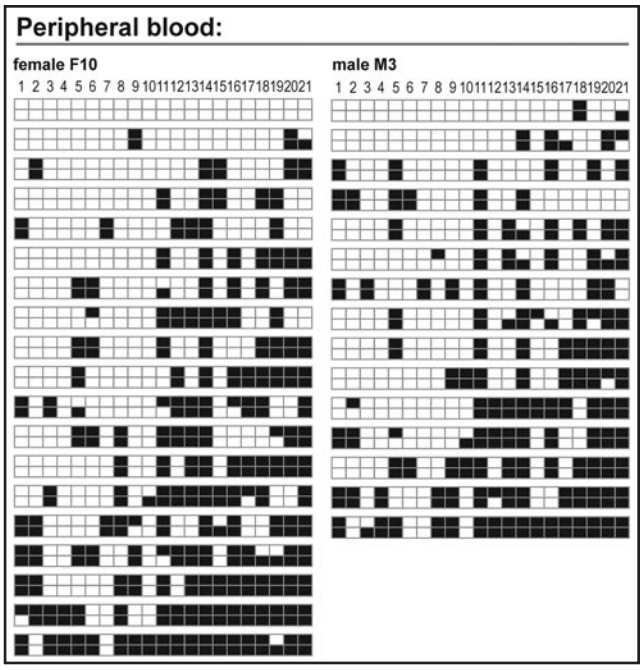


Figure 3. *LEP* promoter methylation in human peripheral blood leukocytes. 21 complementary CG dinucleotides were analyzed by hairpin-bisulfite PCR on both strands of individual DNA molecules. The two rows of boxes within each rectangle represent CG sites on either the top or the bottom strand of an individual, double-stranded DNA molecule. Unmethylated CGs are shown in white; methylated CGs are shown in black. The sequences obtained from each tissue are sorted by methylation density. Numbers correspond with the 21 CGs of the human sequence depicted in Figure 1B.

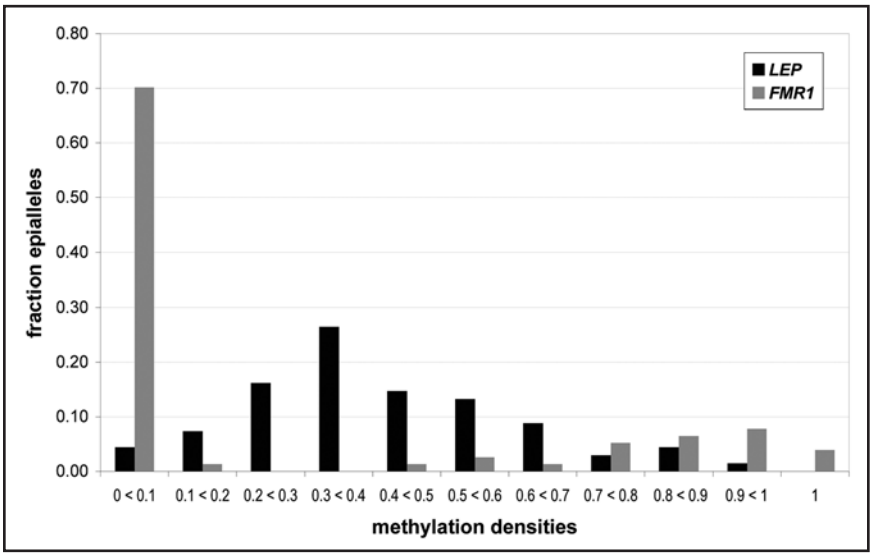


Figure 4. Methylation densities of *LEP* and *FMR1* in peripheral blood leukocytes. Epialleles were sorted into 11 groups by ascending methylation densities and their relative abundance and distribution plotted. The epialleles from a male and a female were pooled to provide the *LEP* data set (see also Fig. 3); methylation patterns from top and bottom strands of hairpin PCR products were treated as individual epialleles (n = 68). Epialleles of the *FMR1* CpG island have been described previously25 and comprise data from three females (n = 77). *FMR1* is an X Chromosome-linked gene and epialleles originated from either active/unmethylated or, inactive/densely methylated X chromosomes in female PBLs. The distributions of methylation densities for *Fmr1* and *Lep* epialleles were found to differ significantly by the two-sample Kolmogorov-Smirnov test ($p < 0.0001$).

Methylation data collected in the past from the *FMR1* promoter on inactive X-alleles in female cells[25] enabled comparison with methylation data of the *LEP* promoter, since DNA from PBLs was used for the analysis of both genes. The broad distribution of methylation densities within the population of *LEP* epialleles is significantly different and contrasts sharply with the bimodal distribution of *FMR1* epialleles, whose methylation densities correlate to the stable on-off expression states of *FMR1* (Fig. 4). CpG island methylation typically indicates permanent gene silencing, and is thought to prevent efficient gene reactivation.[11,28] Overall, the moderate and low levels of promoter methylation detected in human adipose tissues and PBLs suggests that the epigenetic state of *LEP* is generally less stable, perhaps facilitating transitions between active and inactive expression states during the life time of a cell or tissue. Rather than an "on-off" switch, the broad spectrum of methylation densities evokes comparison with a dimmer switch, where methylation density of an epiallele may reflect, or even modulate, the expression level of *LEP*.

Melzer and colleagues have demonstrated that methylation indeed can modulate or silence the activity of the *LEP* promoter when driving the expression of a luciferase reporter gene in a human adipose cell line.[21] Their results showed that luciferase activity from the partially-methylated *LEP* promoter was reduced by one-third relative to activity from the unmethylated promoter. Three specific CG sites within the minimal *LEP* promoter region were found to play an important role in regulating reporter gene expression;[21] Methylation of a CG located within the C/EBP-binding motif caused a decrease in promoter activity, and methylation of two CG sites proximal to the TATA-box strongly diminished expression of the luciferase reporter.[21] The in vivo methylation status of these three CG sites is reported here, as they correspond to CG sites 11, 12 and 13 within the analyzed region of the human *LEP* promoter (see Figs. 1B, 2, 3 and 6). It is apparent that CG sites 11 to 21 are by and large methylated at higher frequency, than are CG sites 1 to 10 (see Figs. 2, 3). CG site 11 is of interest since methylation could affect binding and activity of C/EBP-α,[21] a transcription factor that is known to modulate expression of *LEP*.[18,29] CG site 11 is methylated at a high frequency (77%), when compared to the regional average (43%) in methylated PBL-epialleles. Similarly, 43% of methylated epialleles from fat tissue are modified at CG site 11, whereas the regional average of methylation density is only 23%. The incidence of methylation at the C/EBP-α binding site is particularly striking in sparsely methylated epialleles from fat tissue, since only one or few additional cytosines appear to remain methylated, along with CG site 11 (Fig. 2). Further research is warranted to determine how methylation density of a given *LEP* epiallele in vivo correlates with: (1) the modification of histones surrounding the promoter and (2) transcription levels of *LEP* RNA.

The mouse *Lep* promoter was analyzed in four somatic tissues. In fat tissue, a mosaic pool of unmethylated and densely methylated *Lep* epialleles was detected (Fig. 5). Cells from brain, liver and spleen carry *Lep* epialleles that are hypermethylated in most cases (Fig. 5). The current data provide evidence that

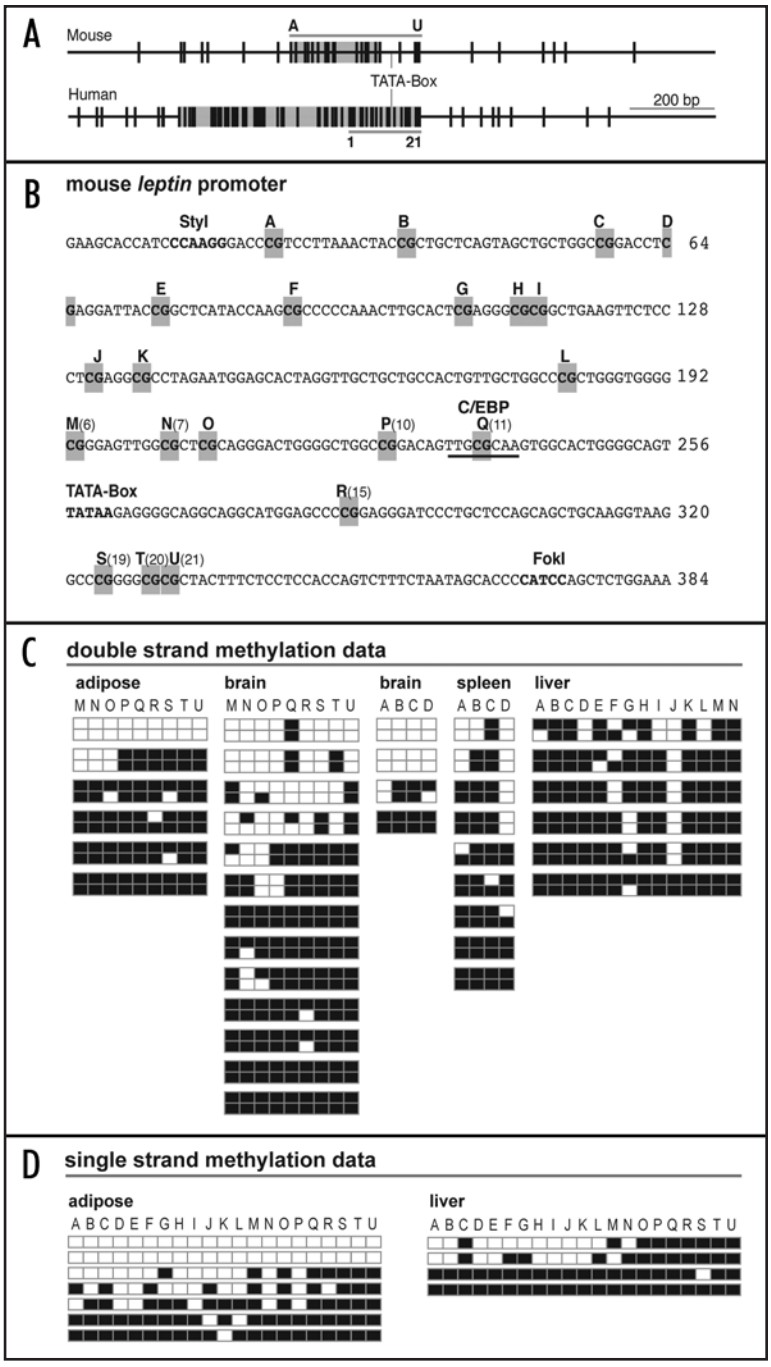


Figure 5. Region of the mouse Leptin promoter. (A) Plots show the distribution of CG dinucleotides—potential sites of cytosine methylation—within a 1.5 kb genomic region centered around the TATA-box promoter element. DNA segments meeting criteria of CpG islands are depicted in gray. The human *LEP* CpG island is shown for comparison. Gray lines show the location of analyzed CGs within the two CpG islands. (B) Sequence of the mouse *Lep* promoter with CG sites highlighted in gray. Letters A to U were assigned to each of the analyzed CGs; numbers in parenthesis indicate the orthologous CG position in the human sequence (see also Fig. 1B). Target sites for restriction enzymes StyI and FokI, which were used for ligation of hairpin linkers are indicated. (C) Double stranded DNA methylation data were obtained from mouse adipose, liver, brain and spleen tissues by hairpin bisulfite PCR. Various combinations of hairpin linkers and PCR primers were used, enabling examination of different numbers of CG sites within the promoter. The two rows of boxes within each rectangle represent CG sites on either the top or the bottom strand of an individual, double-stranded DNA molecule. Unmethylated CGs are shown in white; methylated CGs are shown in black. The sequences obtained from each tissue are sorted by methylation density. Letters above the boxes refer to the positions of CG dinucleotides within the sequence of the mouse Lep promoter as shown in (B). (D) Methylation patterns obtained by conventional, single strand bisulfite sequencing of the "top" DNA strand of the *Lep* promoter. DNA from adipose tissue and liver was analyzed. Each row of boxes represents the CG sites of an individual DNA strand; unmethylated CGs are depicted by white boxes, while methylated CGs are depicted by black boxes.

methylation densities are significantly different between human *LEP* and mouse *Lep*; murine epialleles are overall more densely methylated than their human orthologues ($p < 0.001$; $\chi^2 = 446$, df = 3). This finding suggests that the mouse *Lep* gene may have a higher probability of acquiring dense methylation patterns, which generally correlate with gene silencing.

DNA methylation established at particular genomic loci can be transmitted to offspring.[30-33] Thus, I was curious to assess *LEP* methylation status in human sperm DNA. With a single exception, the sampled sperm epialleles were all unmethylated (12), or had a single methylated CG site (2) (Fig. 6). The lone densely methylated epiallele likely derived from a somatic cell that was isolated along with spermatozoa, but the possibility that this sequence came from a gametic cell cannot be excluded. Likewise, predominantly hypomethylated *Lep* epialleles were recovered from mouse sperm, clearly distinguishing this cohort of molecules from somatic tissue sequences (Fig. 6). A few methylated *Lep* sequences (5) were also detected in the mouse sperm DNA sample, but ascertainment of their somatic or gametic origin was not possible (Fig. 6). The data from human and mouse sperm suggest that the *LEP* promoter becomes reprogrammed by demethylation during male gametogenesis. Since there is no indication that *LEP/Lep* carries a parental- specific imprint, and this locus is generally unmethylated in spermatozoa, de novo methylation of the promoter most often is expected to occur in somatic cells, after fertilization.

While most germ cells have unmethylated *LEP* epialleles, it is conceivable that some of the sperm cells could carry methylated versions of the *LEP* promoter. Evidence that the methylation state of a gene can vary in the male germ line is provided by results of recent studies, where intra- and interindividual methylation differences were identified in humans.[33,34] Future experiments are required to determine whether transgenerational inheritance of methylated *LEP* epialleles is possible.

Methylation in the germline would be expected to deplete the *Leptin* promoter of CG dinucleotides over time. Methylated cytosines tend to deaminate at higher frequencies than do unmethylated cytosines, and thereby promote evolutionary C → T and G →A base transitions.[35,36] I compared 1500 bp of orthologous, genomic sequence surrounding the mouse and human *Lep/LEP* promoters, and observed a 58% lower density of CG dinucleotides in mouse (34 CGs vs. 81 CGs). Furthermore, the 216 bp mouse CpG island is almost three times smaller than the 625 bp human CpG island sequence (Figs. 1A and 5A). The core of the *Lep/LEP* promoters is conserved, but numerous CGs in the human sequence are occupied in mouse by TG or CA dinucleotides at the equivalent location; these are likely deamination products of methylated cytosines (Fig. 1B). The "sinking" CpG island in mouse suggests that methylated

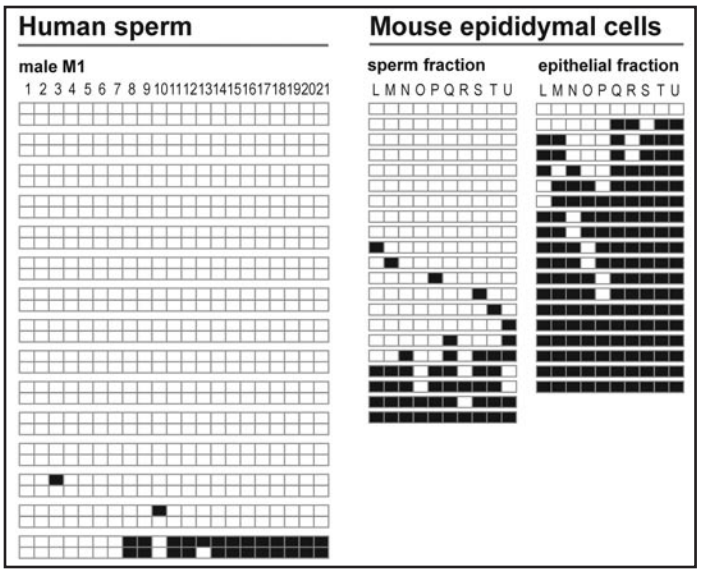


Figure 6. Methylation status of the *Leptin* promoter in mature sperm. The human *LEP* promoter: 21 complementary CG dinucleotides were analyzed by hairpin-bisulfite PCR on both strands of individual DNA molecules. The two rows of boxes within each rectangle represent CG sites on either the top or the bottom strand of an individual, double-stranded DNA molecule. Unmethylated CGs are shown in white; methylated CGs are shown in black. The sequences obtained from each tissue are sorted by methylation density. Numbers correspond with the 21 CGs of the human sequence depicted in Figure 1B. The mouse Lep promoter: conventional bisulfite sequencing was used because it permits PCR amplification from limited amounts of DNA; conditions are less stringent using the conventional bisulfite sequencing protocol and, therefore, less DNA is destroyed during the procedure. Each row of boxes represents CG sites of an individual DNA strand; unmethylated CGs are depicted by white boxes, while methylated CGs are depicted by black boxes. Letters above the boxes refer to the positions of CG dinucleotides within the *Lep* promoter sequence as shown in Figure 5B. In order to analyze methylation patterns on DNA from mature mouse sperm, cells isolated from the epididymis were separated into a spermatozoa-enriched fraction and a spermatozoa-depleted fraction (see Methods). Methylation data are shown from both fractions; the spermatozoa-enriched fraction is labeled "sperm" and the spermatozoa-depleted fraction is labeled "epithelial".

*Lep* epialleles are present in the germline at a higher frequency than their human orthologs. Depletion of CG dinucleotides is not restricted to the *Lep* CpG island, and appears to affect many CpG islands in the mouse genome.[37,38] The question whether increased methylation, as observed for the murine *Lep* promoter in somatic tissues, is a genome-wide phenomenon in mouse, and a contributing factor to the accelerated loss of CpG islands in rodent cells, calls for comparative epigenomic studies.

In summary, the analysis of somatic and gametic cells demonstrated that the *LEP* CpG island constitutes a T-DMR, and that the promoter is subject to dynamic, epigenetic programming in human and in mouse. Expression of this metabolic gene therefore has the potential to be modulated by DNA methylation, raising an abundant number of intriguing biologically and clinically relevant questions. Identification of in vivo methylation at the *LEP* promoter provides a molecular entry point to study the timing, factors and conditions that lead to tissue-specific methylation patterns of gene promoters.

**Note added in proof:** In a recent study Collas and colleagues also report mosaic cytosine methylation of the *LEP* promoter in human adipose tissue (Noer A, Sørensen AL, Boquest AC, Collas P.; Stable CpG hypomethylation of adipogenic promoters in freshly isolated, cultured, and differentiated mesenchymal stem cells from adipose tissue. Mol Biol Cell 2006; 17:3543-56.)

**References**


1. Swartz MN, Trautner TA, Kornberg A. Enzymatic synthesis of deoxyribonucleic acid. XI. Further studies on nearest neighbor base sequences in deoxyribonucleic acids. J Biol Chem 1962; 237:1961-7.
2. Russell GJ, Walker PM, Elton RA, Subak-Sharpe JH. Doublet frequency analysis of fractionated vertebrate nuclear DNA. J Mol Biol 1976; 108:1-23.
3. Bird AP. CpG-rich islands and the function of DNA methylation. Nature 1986; 321:209-13.
4. Rollins RA, Haghighi F, Edwards JR, Das R, Zhang MQ, Ju J, Bestor TH. Large-scale structure of genomic methylation patterns. Genome Res 2006; 16:157-63.
5. Marino-Ramirez L, Spouge JL, Kanga GC, Landsman D. Statistical analysis of over-represented words in human promoter sequences. Nucleic Acids Res 2004; 32:949-58.
6. Saxonov S, Berg P, Brutlag DL. A genome-wide analysis of CpG dinucleotides in the human genome distinguishes two distinct classes of promoters. Proc Natl Acad Sci USA 2006; 103:1412-7.
7. Shiota K, Kogo Y, Ohgane J, Imamura T, Urano A, Nishino K, Tanaka S, Hattori N. Epigenetic marks by DNA methylation specific to stem, germ and somatic cells in mice. Genes Cells 2002; 7:961-9.
8. Song F, Smith JF, Kimura MT, Morrow AD, Matsuyama T, Nagase H, Held WA. Association of tissue-specific differentially methylated regions (*TDMs*) with differential gene expression. Proc Natl Acad Sci USA 2005; 102:3336-41.
9. Khulan B, Thompson RF, Ye K, Fazzari MJ, Suzuki M, Stasiek E, Figueroa ME, Glass JL, Chen Q, Montagna C, Hatchwell E, Selzer RR, Richmond TA, Green RD, Melnick A, Greally JM. Comparative isoschizomer profiling of cytosine methylation: The HELP assay. Genome Res 2006.
10. Stein R, Gruenbaum Y, Pollack Y, Razin A, Cedar H. Clonal inheritance of the pattern of *DNA* methylation in mouse cells. Proc Natl Acad Sci USA 1982; 79:61-5.
11. Siegfried Z, Eden S, Mendelsohn M, Feng X, Tsuberi BZ, Cedar H. DNA methylation represses transcription in vivo. Nat Genet 1999; 22:203-6.
12. Schubeler D, Lorincz MC, Cimbora DM, Telling A, Feng YQ, Bouhassira EE, Groudine M. Genomic targeting of methylated DNA: Influence of methylation on transcription, replication, chromatin structure, and histone acetylation. Mol Cell Biol 2000; 20:9103-12.
13. Bird A. DNA methylation patterns and epigenetic memory. Genes Dev 2002; 16:6-21.
14. Meehan RR. DNA methylation in animal development. Semin Cell Dev Biol 2003; 14:53-65.
15. Lee JT. Molecular links between X-inactivation and autosomal imprinting: X-inactivation as a driving force for the evolution of imprinting? Curr Biol 2003; 13:R242-54.
16. Zhang Y, Proenca R, Maffei M, Barone M, Leopold L, Friedman JM. Positional cloning of the mouse obese gene and its human homologue. Nature 1994; 372:425-32.
17. Friedman JM, Halaas JL. Leptin and the regulation of body weight in mammals. Nature 1998; 395:763-70.
18. Miller SG, De Vos P, Guerre-Millo M, Wong K, Hermann T, Staels B, Briggs MR, Auwerx J. The adipocyte specific transcription factor *C/EBPalpha* modulates human ob gene expression. Proc Natl Acad Sci USA 1996; 93:5507-11.
19. Hwang CS, Mandrup S, MacDougald OA, Geiman DE, Lane MD. Transcriptional activation of the mouse obese (*ob*) gene by *CCAAT*/enhancer binding protein alpha. Proc Natl Acad Sci USA 1996; 93:873-7.
20. Yokomori N, Tawata M, Onaya T. DNA demethylation modulates mouse leptin promoter activity during the differentiation of 3T3-L1 cells. Diabetologia 2002; 45:140-8.
21. Melzner I, Scott V, Dorsch K, Fischer P, Wabitsch M, Bruderlein S, Hasel C, Moller P. Leptin gene expression in human preadipocytes is switched on by maturation-induced demethylation of distinct CpGs in its proximal promoter. J Biol Chem 2002; 277:45420-7.
22. Antequera F, Boyes J, Bird A. High levels of de novo methylation and altered chromatin structure at CpG islands in cell lines. Cell 1990; 62:503-14.
23. Laird CD, Pleasant ND, Clark AD, Sneeden JL, Hassan KM, Manley NC, Vary Jr JC, Morgan T, Hansen RS, Stöger R. Hairpin-bisulfite PCR: Assessing epigenetic methylation patterns on complementary strands of individual DNA molecules. Proc Natl Acad Sci USA 2004; 101:204-9.
24. Miner BE, Stöger R, Burden AF, Laird CD, Hansen RS. Molecular barcodes detect redundancy and contamination in hairpin-bisulfite PCR. Nucleic Acids Res 2004; 32:e135.
25. Stöger R, Kajimura TM, Brown WT, Laird CD. Epigenetic variation illustrated by DNA methylation patterns of the fragile-X gene *FMR1*. Hum Mol Genet 1997; 6:1791-801.
26. Gartler SM, Riggs AD. Mammalian X-chromosome inactivation. Annu Rev Genet 1983; 17:155-90.
27. Lorincz MC, Schubeler D, Hutchinson SR, Dickerson DR, Groudine M. DNA methylation density influences the stability of an epigenetic imprint and Dnmt3a/b-independent de novo methylation. Mol Cell Biol 2002; 22:7572-80.
28. Feng YQ, Desprat R, Fu H, Olivier E, Lin CM, Lobell A, Gowda SN, Aladjem MI, Bouhassira EE. DNA methylation supports intrinsic epigenetic memory in mammalian cells. PLoS Genet 2006; 2:e65.
29. Mason MM, He Y, Chen H, Quon MJ, Reitman M. Regulation of leptin promoter function by Sp1, C/EBP, and a novel factor. Endocrinology 1998; 139:1013-22.

30. Stöger R, Kubicka P, Liu CG, Kafri T, Razin A, Cedar H, Barlow DP. Maternal-specific methylation of the imprinted mouse *Igf2r* locus identifies the expressed locus as carrying the imprinting signal. Cell 1993; 73:61-71.
31. Jacobsen SE, Meyerowitz EM. Hypermethylated SUPERMAN epigenetic alleles in arabidopsis. Science 1997; 277:1100-3.
32. Cubas P, Vincent C, Coen E. An epigenetic mutation responsible for natural variation in floral symmetry. Nature 1999; 401:157-61.
33. Suter CM, Martin DI, Ward RL. Germline epimutation of MLH1 in individuals with multiple cancers. Nat Genet 2004; 36:497-501.
34. Flanagan JM, Popendikyte V, Pozdniakovaite N, Sobolev M, Assadzadeh A, Schumacher A, Zangeneh M, Lau L, Virtanen C, Wang SC, Petronis A. Intra- and interindividual epigenetic variation in human germ cells. Am J Hum Genet 2006; 79:67-84.
35. Sved J, Bird A. The expected equilibrium of the CpG dinucleotide in vertebrate genomes under a mutation model. Proc Natl Acad Sci USA 1990; 87:4692-6.
36. Kondrashov AS. Direct estimates of human per nucleotide mutation rates at 20 loci causing Mendelian diseases. Hum Mutat 2003; 21:12-27.
37. Antequera F, Bird A. Number of *CpG* islands and genes in human and mouse. Proc Natl Acad Sci USA 1993; 90:11995-9.
38. Zhao Z, Zhang F. Sequence context analysis in the mouse genome: Single nucleotide polymorphisms and CpG island sequences. Genomics 2006; 87:68-74.